TECHNICAL PAPER

JOURNAL OF THE SOUTH AFRICAN INSTITUTION OF CIVIL ENGINEERING
ISSN 1021-2019
Vol 61 No 2, June 2019, Pages 2–20, Paper 1735

Evaluation of empirical equations to predict bridge pier scour in a non-cohesive bed under clear-water conditions

J K Vonkeman, G R Basson

Pier scour has been cited as the main mechanism responsible for the failure of bridges spanning rivers. Despite extensive research since the 1950s, there is no universally agreed upon procedure to accurately predict the equilibrium scour depth. Experimental data was generated by 48 tests with four flows and three pier shapes to evaluate the capability of 30 empirical equations to predict the local scour depth. Fine sand and crushed peach pips were used to address the scaling challenges of the equations by means of an equivalent movability number. The equations yielded a wide range of mostly unreliable results, particularly for the non-cylindrical pier shapes. Nevertheless, the HEC-18 models are recommended, in conjunction with Shen *et al* (1969), and Ali and Karim (2002), because they rely on the pier Reynolds number, a parameter which is significant in the vortex formation. Prediction models taking the horseshoe vortex into consideration could offer better scour depth predictions. Field data was analysed to improve the HEC-18 equation with new factors for pier shape and armouring for different confidence intervals. The armouring factor is based on the particle Reynolds number as opposed to the widely adopted critical velocity, and achieves considerably less scatter about the line of equality despite under-predictions for the cylindrical piers. Alternatively, a diagram comparable to the Modified Liu Diagram has the potential to predict bridge pier scour even though the pier structure parameters are omitted. Further research and improved prediction models should be considered, particularly advanced numerical models which are becoming increasingly feasible.

JEANINE K VONKEMAN, who is an Associate Member of SAICE, is a postgraduate student in Hydraulic Engineering at Stellenbosch University. She completed her BEng (*cum laude*) in Civil Engineering at the University of Pretoria in 2014 and is currently working towards a PhD on a numerical model for bridge pier scour, which was upgraded from her MEng degree.

Contact details:
PhD Civil Engineering Student
Stellenbosch University
Private Bag X1
Matieland 7602
South Africa
T: +27 83 286 8760
E: jkvonkeman@gmail.com / jvonkeman@sun.ac.za

PROF GERRIT R BASSON Pr Eng, who is a Member of SAICE, is a professor in Hydraulic Engineering in the Civil Engineering Department at Stellenbosch University. He obtained a PhD from Stellenbosch University in 1996 and has more than 30 years' experience mainly in the fields of river hydraulics, fluvial morphology and the design of large hydraulic structures. He has worked on projects in 21 countries.

Contact details:
Professor in Hydraulic Engineering
Department of Civil Engineering
Stellenbosch University
Private Bag X1
Matieland 7602
South Africa
T: +27 21 808 4355
E: grbasson@sun.ac.za

Keywords: pier scour, empirical equations, clear-water, alluvial, Reynolds number

BACKGROUND

The placement of a bridge pier in a hydraulic environment changes the flow field, yielding it susceptible to local scour whereby the surrounding sediment is washed away by swiftly moving water. As a result, the bridge foundation may be undermined and the structural stability compromised. In fact, local scour at piers has been cited as the main mechanism responsible for the collapse of bridges founded in alluvial beds (Deshmukh & Raikar 2014). Huber (1991) and Sumer (2007) estimate that 60% of all structural bridge failures can be attributed to scouring and not to overloading. Extensive research has been conducted on the prediction of bridge pier scour depth since the 1950s, and yet there is no universally agreed upon procedure to accurately predict the equilibrium scour depth (Rooseboom 2013).

Most scour equations traditionally used in bridge designs have been developed on the basis of experimentation, dimensional analyses and simplified theoretical models. The equations have been derived by assuming dominant parameters, reducing them to simplified relationships and then calibrating them by means of a coefficient from laboratory and field data.

The comparison of different empirical equations has been the topic of many studies. Johnson (1995) used field data to evaluate the accuracy of seven pier scour equations. Landers and Mueller (1996) analysed five selected equations with field data. Gaudio *et al* (2010) tested six formulae by using original field data and synthetic data produced by the Monte Carlo technique. In more recent studies, Toth (2015) evaluated ten different equations. One of the most comprehensive studies is that of Sheppard *et al* (2014) who evaluated 23 equations for under-prediction using compiled laboratory and field databases. The equations were then combined to produce the Sheppard & Melville Model. Similarly, Mueller (1996) and Mueller

Vonkeman JK, Basson GR. Evaluation of empirical equations to predict bridge pier scour in a non-cohesive bed under clear-water conditions. J. S. Afr. Inst. Civ. Eng. 2019:61(2), Art. #1735, 19 pages. http://dx.doi.org/10.17159/2309-8775/2019/v61n2a1

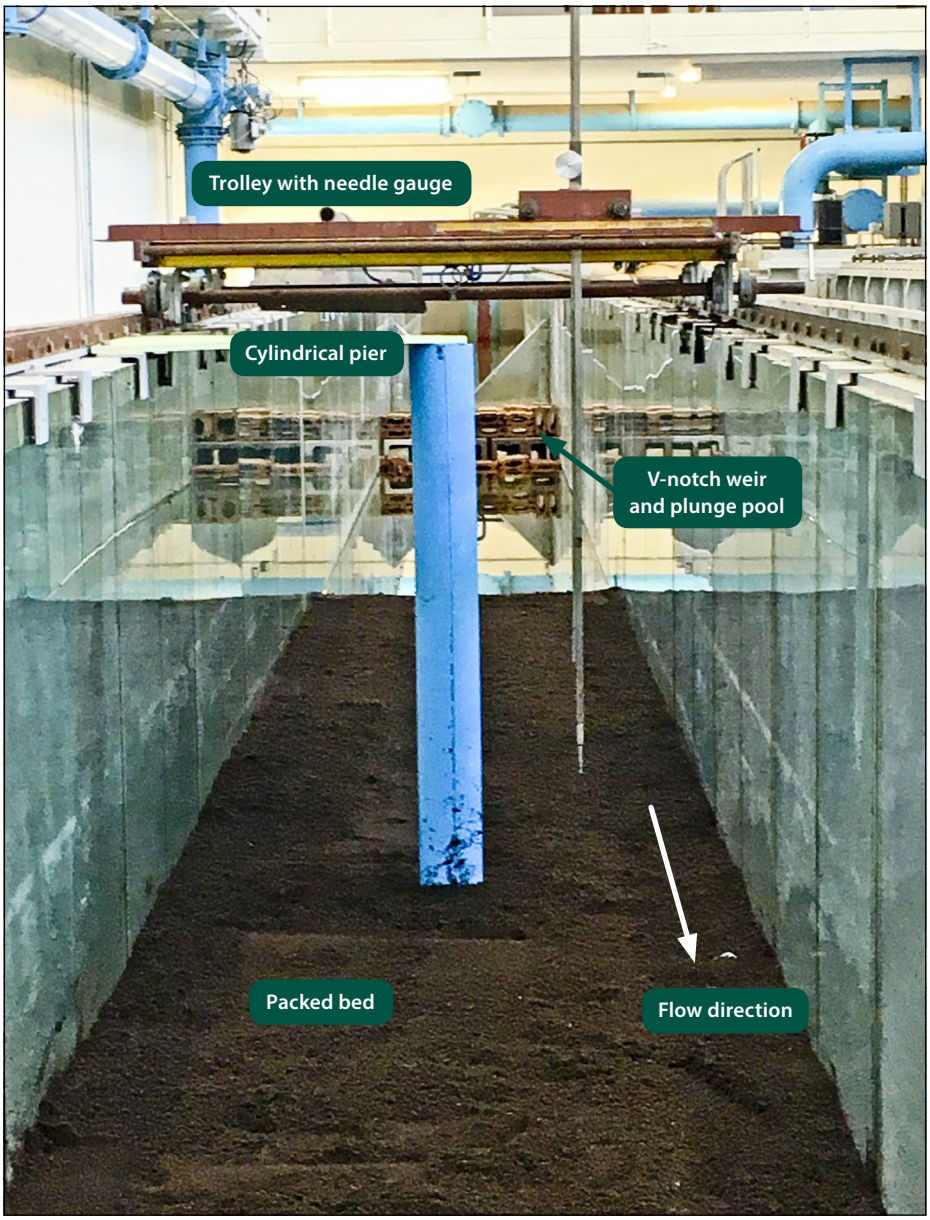

Figure 1 Photo of the laboratory flume setup with cylindrical pier and sediment bed

and Wagner (2005) evaluated 22 and 26 equations respectively, and improved the HEC-18 method. The comparative studies are based on statistical analyses using, amongst others, percentage error, residuals, standard deviation, bias or rankings. Without exception, the authors all concluded that the various empirical equations produce significantly different predictions from the field and that further research is required. Furthermore, the following conclusions were also recurring:

- The equations produce results that are not only different from the field or laboratory, but are in weak agreement with one another. The equations are not universal and only yield good results under conditions similar to those from which they were derived.
- Most of the formulae overestimate observed scour depths and may perform better in conservative designs. However, this leads to uneconomical designs of unnecessarily expensive foundations or countermeasures. On the other hand, some of the formulae are not fit for pier design due to under-predictions, for example Froelich (1988).
- Generally, it appears that the HEC-18 formulae by the US Federal Highway Administration (FHWA) are favoured for results that most closely resemble the field and rarely under-predict scour depth. It is also known as the CSU (Colorado State University) equation with modifications in the form of coefficients for the effect of the bed material. The Shen *et al* (1969) model, one of the equations upon which the HEC-18 formula was based, relies on the pier Reynolds number and also performed well in the literature study.
- Further research and improved models are recommended (Arneson *et al* 2012).

The intention of this study was to simulate bridge pier scour in a laboratory and to gain an understanding of the scouring process. The data generated by the physical modelling was then applied to evaluate different methods for predicting the equilibrium scour depth. The objective was to demonstrate the shortcomings of thirty of the better-known empirical equations and to emphasise the need for improved prediction methods to pave the way for future research on numerical modelling. A summary of the different methods is presented in the Appendix to this paper. Finally, field data was analysed to generate a new equation based on the particle Reynolds number as opposed to the widely adopted critical velocity.

EXPERIMENTAL WORK

Experimental work was conducted at the Civil Engineering Hydraulics Laboratory, Stellenbosch University, in a rectangular flume with a 40 m length, 1 m width and 1.24 m depth. A sediment bed was packed in the flume around a scaled pier model, and water was released to emulate channel flow and local scouring. The tests were performed for subcritical flow under clear-water conditions (Froude number $Fr < 0.26$ and critical velocity ratio $v/vc < 1$) and for a constant water depth $y = 0.2$ m which was manually controlled with a sluice gate at the downstream end of the flume. A V-notch weir controlled the inflow and a plunge pool with tubes aligned the flow to ensure that uniform, fully developed flow would reach the pier after a 9 m entrance length. Figure 1 shows a photograph of the experimental setup.

A total of 48 different tests were conducted whereby a combination of four different flows, three pier shapes and two sediment materials was used. The three different pier shapes included a cylindrical pier, a round-nosed pier and a sharp-nosed pier, as indicated in Figure 2. The pier models were designed based on a model-to-prototype scale of 1:15 with a diameter (or width) D of 110 mm and a length L/D ratio of 7. The different inflows that were tested had approach velocities of 0.28, 0.31, 0.34 and 0.37 m/s for the fine sand material, while those for the crushed peach pips were 0.14, 0.17, 0.20 and 0.23 m/s.

The submerged scour pattern that formed in the vicinity of the scaled pier model was manually surveyed and the flow pattern was visualised by Acoustic Doppler

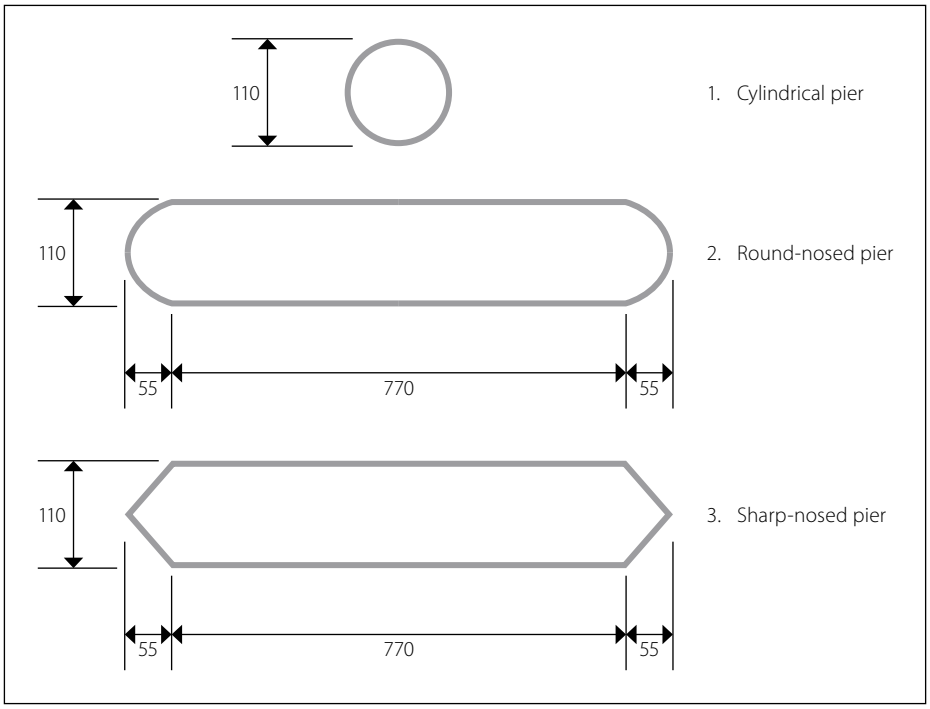

Figure 2 The different pier shapes with dimensions

Velocimetry (ADV) measurements. Furthermore, the flow field was measured for the flume setup without sediment, i.e. a fixed bed to simulate rigid plane-bed flow. Ten percent of the experiments were duplicated three times to ensure repeatability of the results, and showed a maximum deviation of 9%.

Model-to-prototype scaling

Empirical equations are formulated specifically for full-scale field applications with sediment, such as sand with a relative density of 2.6. Consequently, equations developed from physical models are faced with scaling challenges whereby they overestimate the actual scour field depths (Lee & Sturm 2009). Sediment transport problems are normally modelled by applying Froude similarity, and the median grain size is scaled according to the Shields' criterion (Heller 2011). This may result in a very small model sediment size that exhibits cohesive inter-particle forces not present in sand bed rivers (Lee & Sturm 2009). According to FHWA (Arenson *et al* 2012), "it is not possible to scale the bed material size". Heller (2011) recommends that a sediment with a smaller density and larger grain diameter should be employed to incorporate the non-scalable effects of the hydraulic forces in the settling velocity and density. Thus, crushed peach pips, albeit a biomaterial, were used to more accurately replicate alluvial sediment in the field.

The material properties measured for the two sediments, presented in Table 1, were the median particle size d, maximum theoretical relative density MTRD or s, angle of repose ϕ, settling velocity w and critical velocity v_c. Both sediment beds may be classified as uniformly graded based on the particle size distributions $\sigma_g = (d_{84}/d_{16})^{0.5} < 2$. These values were obtained from standard sieve analyses, rice density tests, fixed funnel tests and settling column tests.

Rooseboom *et al* (1983) argue that particle size poorly represents the transportability of sediment and instead recommend the use of settling velocity. The Modified Liu Diagram in Figure 3 (based on Rooseboom *et al* 1983) was generated to obtain an identical movability number, and thereby scale the density and particle sizes for the peach pips to that of a representative in-situ alluvial sediment (refer to Table 1). The movability number (or stream power) and the particle Reynolds number are defined in Equations 1 and 2 respectively.

$$\frac{v^*}{w} = \frac{\sqrt{gy_1 S_f}}{w} \quad (1)$$

$$Re_p = \frac{\sqrt{gy_1 S_f}\, d}{\nu} \quad (2)$$

where S_f is the energy slope, g is the gravitational acceleration and ν is the kinematic viscosity. Equation 3 was used to relate the particle density and size with settling velocity. Several different approximations for the coefficient exist, but a value of 1.1 is recommended C_D for the scaling of rough sediment particles > 1 mm, while Stoke's Law should be applied for particles < 0.1 mm (Van Rijn 1987) and Zanke (1977) to particles < 1 mm.

Table 1 Sediment characteristics measured for the fine sand and crushed peach pips

Properties	d_5 (mm)	σ_g	MTRD	φ_{sat}	φ_{dry}	w_5 (m/s)	v_c (m/s)	Scaled d (mm)	Scaled MTRD
Fine sand	0.214	1.36	2.63	45°	28°	0.036	0.375	3.21	2.63
Peach pips	0.740	1.57	1.28	44°	32°	0.032	0.225	1.87	2.63

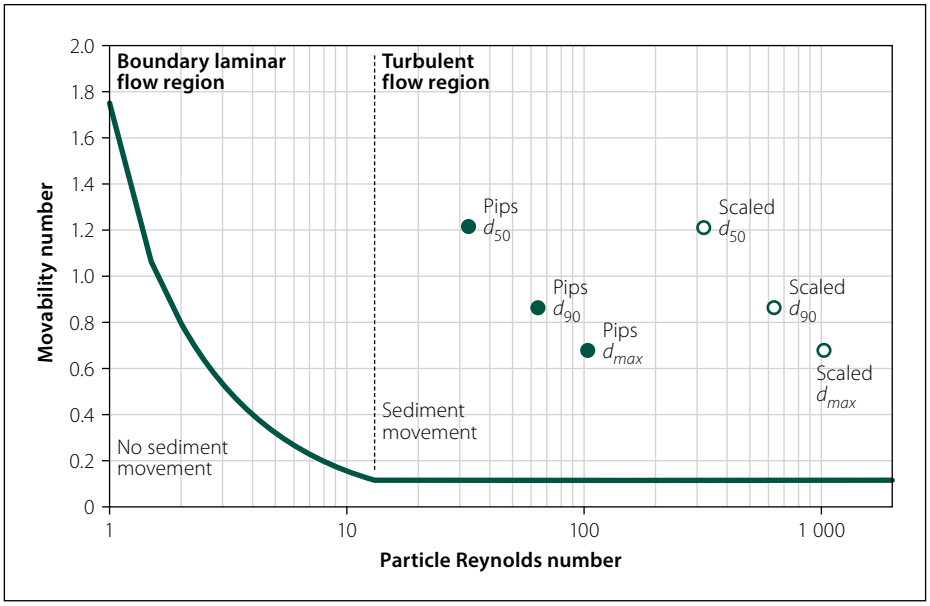

Figure 3 Modified Liu Diagram to scale peach pips

Table 2 Critical flow velocities (m/s) determined by empirical equations

Equation	Hancu (1971)	Neill (1973)	Gao *et al* (1993)	Richardson & Davis (1995)	Melville (1997)	Sheppard *et al* (2014)	Equation 4
Fine sand	0.276	0.314	0.284	0.283	0.276	0.242	0.328
Peach pips	0.166	0.374	0.170	0.428	0.360	0.302	0.204

$$w = \begin{cases} \sqrt{(\rho_s/\rho - 1)gd}, & d > 1 \text{ mm} \\ \dfrac{C_D\sqrt{(\rho_s/\rho - 1)gd^2}}{18\nu}, & d < 0.1 \text{ mm} \\ 10\nu/d(\sqrt{1 + 0.01d^3} - 1), & 0.1 < d < 1 \text{ mm} \end{cases} \quad (3)$$

where ρ_s and ρ is the density of the sediment and fluid respectively.

Incipient motion

Most of the empirical equations for bridge pier scour rely on incipient motion described empirically by critical velocity. The threshold of movement can also be described in terms of shear stress, settling velocity and stream power. Numerous equations exist to define the critical velocity, and ambiguities exist whereby some of the equations for bridge pier scour fail to reference an appropriate equation to determine the critical velocity (Breusers *et al* 1977; Jain 1981; Sheppard & Miller 2006). The threshold of sediment movement is clearly an important parameter in scour calculations, and yet literature neglects to address that different equations for critical velocity could yield different scour depth predictions. Therefore, critical velocities determined experimentally (see Table 1) were used in the analysis (unless specified otherwise) to ensure that the relative velocity ratio v/v_c was maintained for both model and prototype scales.

The scaling challenge is further demonstrated by the empirical equations which over-predict the critical velocity for the peach pip particles (as shown in Table 2), because they do not account for density, unlike Gao *et al* (1993), Hancu (1971) and Equation 4. It is derived from the Shields diagram that assumes the shear stress limit for incipient motion for Re > 400 is $\tau_c = 0.056(\rho_s - \rho)gd$ (Graf 1971). The Hancu (1971) model for scour depth relies on a critical velocity that is also derived from the Shields diagram and proves to be one of the more accurate scour equations in the subsequent section.

$$v_c = 1.9\sqrt{gd(s-1)}\left\{\frac{R}{d}\right\}^{1/6} \quad (4)$$

where R is the hydraulic radius. The equations used in Table 2 are given in the Appendix.

Time to reach equilibrium

Local scour is a time-dependent process whereby equilibrium is progressively achieved as the scour hole grows and the bed shear stresses near the bed gradually fall below the critical shear stress (Roulund *et al* 2005). Melville and Chiew (1999) believe that the equilibrium depth takes several days or months to develop, while Breusers *et al* (1977) claim that the time to reach equilibrium depth may be infinite. However, flood peaks often do not last long enough to develop an equilibrium scour depth and it is impractical to run an experiment for several days. Owing to the divided notion in literature on the time required to reach equilibrium scour, additional tests were performed to establish a suitable time scale for each test to achieve equilibrium scour.

Figure 4 shows that no significant change was observed in the scour hole depth d_s for both sediment beds after two hours, as was the case for Melville (1975), Roulund *et al* (2005) and Mohammed *et al* (2016). Evidently scour development is rapid in the beginning; 50–80% of the equilibrium scour depth develops within 10% of the time required for equilibrium (Melville & Chiew 1999). Therefore, it was assumed that the equilibrium condition is reached when the increase in scour depth does not exceed 5% of the pier diameter.

The empirical equation proposed by Guo (2014) for a time-dependent scour depth was assessed by curve-fitting it to Figure 4. The equation gave an equilibrium scour depth for the peach pips after seven hours as 1.25 times larger than that observed after three hours in the laboratory. The curve-fitting also indicated that the equilibrium scour depth for the fine sand was achieved after 40 minutes. Of the thirty scour equations considered in the study, the only models that attempt to account for time is that of Melville and Coleman (2000), and Ali and Karim (2002) which employ exponential functions.

The scour process

The complex junction flow associated with bridge pier scour results in the formation of separated flow, lee-wake and horseshoe vortices, as illustrated by the photographs in Figure 5. The horseshoe vortex is the main mechanism responsible for scouring. A down-flow in front of the pier is driven by the strong pressure gradient and the vertical velocity component which rolls up when it comes into contact with the bed. The resulting circulation, flow separation and shear layer scour the hole, comparable to an impinging jet digging up the sediment material. The ends of the system are swept downstream and the sediment is deposited

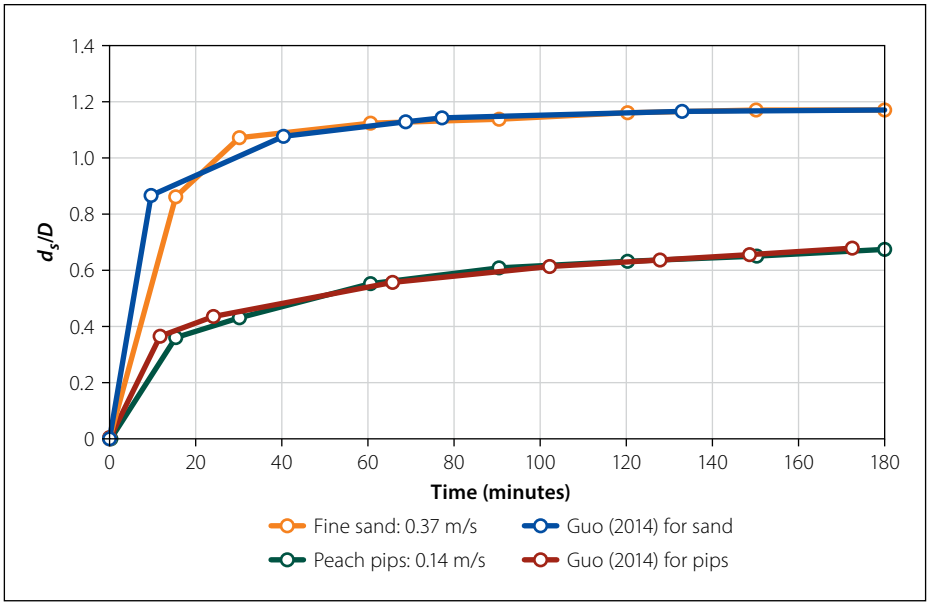

Figure 4 Development of relative scour depth with time in the laboratory

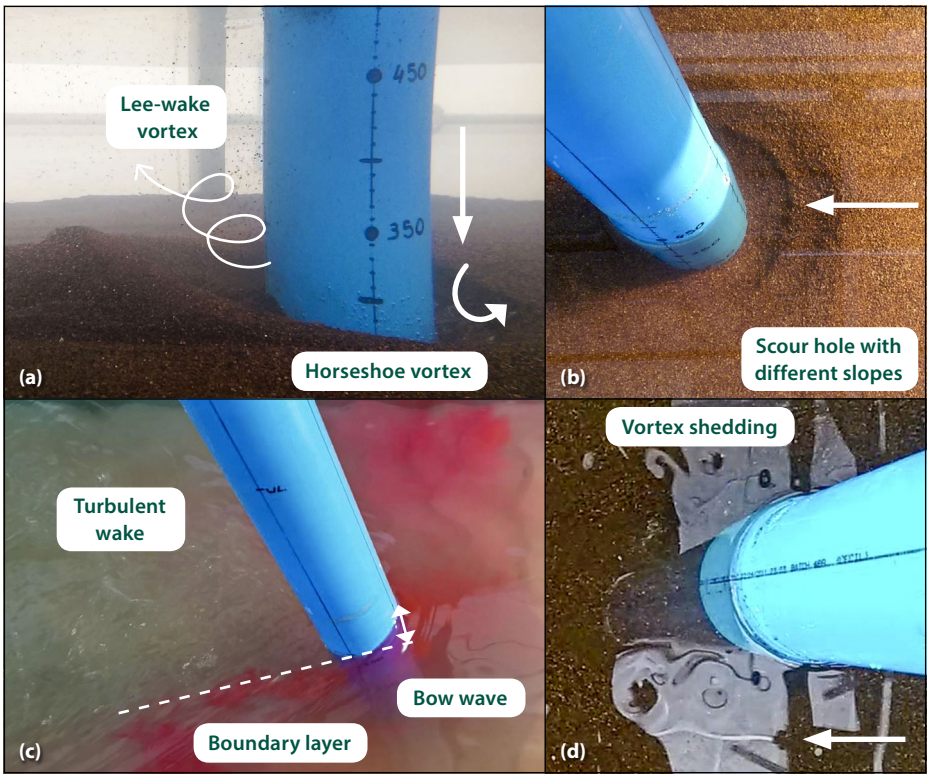

Figure 5 Photographs of the flow pattern elements associated with bridge pier scouring

Table 3 Maximum bridge pier scour depth and extent from experimental work (m)

		Cylindrical pier			Round-nosed pier			Sharp-nosed pier		
	v (m/s)	d_s	l_s	w_s	d_s	l_s	w_s	d_s	l_s	w_s
Fine sand	0.28	0.099	0.15	0.20	0.056	0.16	0.19	0.060	0.17	0.22
	0.31	0.111	0.19	0.24	0.080	0.18	0.22	0.065	0.18	0.25
	0.34	0.114	0.19	0.24	0.094	0.23	0.24	0.084	0.20	0.25
	0.37	0.121	0.25	0.26	0.102	0.25	0.25	0.090	0.20	0.27
Peach pips	0.14	0.063	0.13	0.13	0.037	0.12	0.13	0.009	0.06	0.01
	0.17	0.116	0.21	0.22	0.077	0.17	0.18	0.050	0.13	0.14
	0.20	0.127	0.24	0.28	0.095	0.23	0.25	0.072	0.15	0.20
	0.23	0.135	0.24	0.30	0.111	0.25	0.28	0.106	0.17	0.24

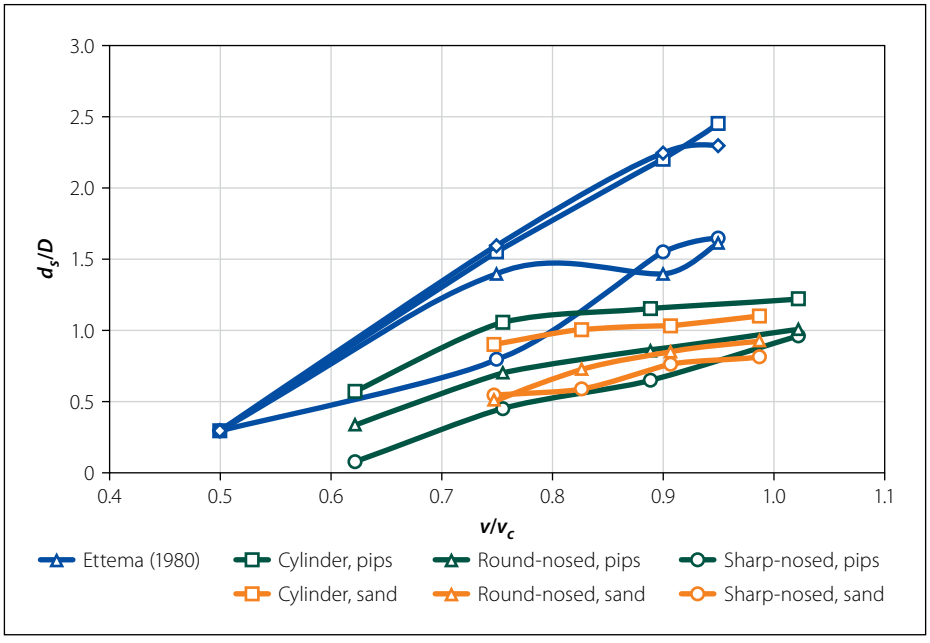

Figure 6 The effect of relative velocity on relative scour depth from experimental work

in the low-pressure zone behind the pier to form the characteristic horseshoe shape.

A bow wave is formed at the free surface in front of the pier caused by an upward flow circulating in a direction opposite to that of the horseshoe vortex. The bow wave has the ability to counteract and weaken the horseshoe vortex only in shallow flow depths.

The slope of the scour hole can be divided into different regions, as demonstrated by Figure 5(b). The primary area is driven by the vortex and bed shear stress, while the secondary area is driven by the slope stability or shear slides with a slope angle approximating that of the saturated angle of repose.

The lee-wake vortex forms behind the pier. As the flow reaches the pier, the velocity decreases abruptly and the flow is deflected away from the pier. The flow accelerates where the streamlines converge and a boundary layer is formed, as observed by the coloured dye wands in Figure 5(c). The lee-wake vortices are caused by the rotation of the boundary layer over the surface of the pier. Unstable shear layers form at the pier surface near the bed, which roll up and detach from either side of the pier at the boundary layer. At low Reynolds numbers < 3.5×10^6, unstable vortices are shed from alternating sides of the pier and are swept downstream (Breusers *et al* 1977). Figure 5(d) shows the lee-wake vortex for a Reynolds number of 80×10^3, a pier Reynolds number of 15×10^3 and a typical Strouhal number of 0.2.

Results for experimental work

Table 3 summarises the unscaled scour depth d_s, length l_s and width w_s results from the experimental work. The maximum scour depth was measured at the upstream nose of the pier where the horseshoe vortex circulates. Generally, the length is $0.47d_s$ and the width is $0.4d_s$.

The local scour process is affected by several different yet interrelated parameters of which the relative velocity, relative sediment size, relative flow depth and time to reach equilibrium scour have been identified as the most significant (Williams 2014). The effect of the approach velocity, pier shape and sediment type on equilibrium scour depth could briefly be examined, but flow depth and pier width were fixed in the experimental work.

Figure 6 illustrates that the relative scour depth increases almost linearly with the relative velocity, in accordance with

Ettema (1980). No local scour pattern was observed below a relative velocity condition of 0.5 in accordance with research such as those by Hancu (1971), Breusers *et al* (1977), Sheppard and Miller (2006), and Sheppard *et al* (2014).

Similarly, the relative scour depth increases with an increasing pier Reynolds number, as shown in Figure 7. The pier Reynolds number Re_D = v*D*/*v* describes the turbulence induced by the pier and not by the channel. It is easily the chief parameter affecting the strength of the horseshoe vortex (Roulund *et al* 2005), and yet it has rarely been described relative to scour depth, even though the horseshoe vortex is directly responsible for causing scour. The pier Reynolds number should be considered a more significant scour parameter, because it describes the combined effect of the pier size and approach velocity on the vortex strength.

From Figure 7 it is evident that the sand required a larger Reynolds number (or velocity) to scour the same sized hole as that for the peach pips. The two sediment materials have a different median particle size, as well as density, and are thus best compared when both parameters are considered. The crushed peach pips are the more easily erodible material, because they have a lower settling velocity and a lower critical velocity.

On the other hand, similarly sized scour holes are formed for the same relative velocity or flow intensity for both materials in Figure 6. This is in accordance with Lee and Strum (2009) who suggest that a similar scour depth should be obtained for the scaled *D*/*d* of 882 for the peach pips and 514 for the sand.

With reference to the figures above, a cylindrical pier yields the largest scour hole, while the sharp-nosed pier yields the least amount of scouring because practically no vorticity is generated at the nose of the streamlined pier (Tseng *et al* 2000). The round-nosed pier causes less scouring than the cylindrical pier due to its increased relative pier length *L*/*D*. Only half of the empirical equations evaluated in this study account for pier shape by incorporating different constants as a shape factor *Ks*. However, the effect of the pier shape on scouring cannot simply be described by a single dimensionless shape factor, as demonstrated by Figure 8, because different gradients exist for the near linear relationships. The curves for different *Ks* values in Figure 8 were generated by applying *Ks* to the curve of the cylindrical pier. It is difficult to mathematically describe the effect of pier shape, but numerical modelling has the ability to overcome this shortcoming.

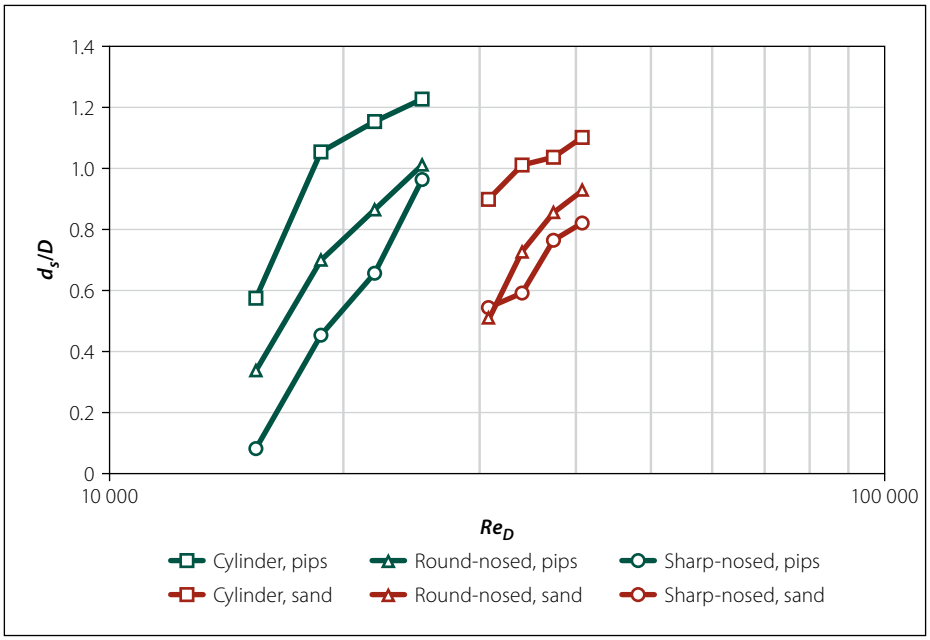

Figure 7 The effect of the pier Reynolds number on the relative scour depth

EVALUATION OF EMPIRICAL EQUATIONS

Thirty empirical equations traditionally employed to predict bridge pier scour were evaluated against the results from the laboratory for a full-scale prototype. The equations were found to yield a wide range of varying and mostly unreliable results for the same case, even under controlled laboratory conditions.

From Figure 9 it is evident that a wide range of scour depths were produced by the equations for each test or boxplot. The scour depth was predominantly over-predicted, as the design equations intend to be conservative when they fail to be accurate. Nevertheless, the empirical equations still predict scour depths varying within a range of 3 m from one another for the same test.

Because empirical equations are generally developed from a standard experimental

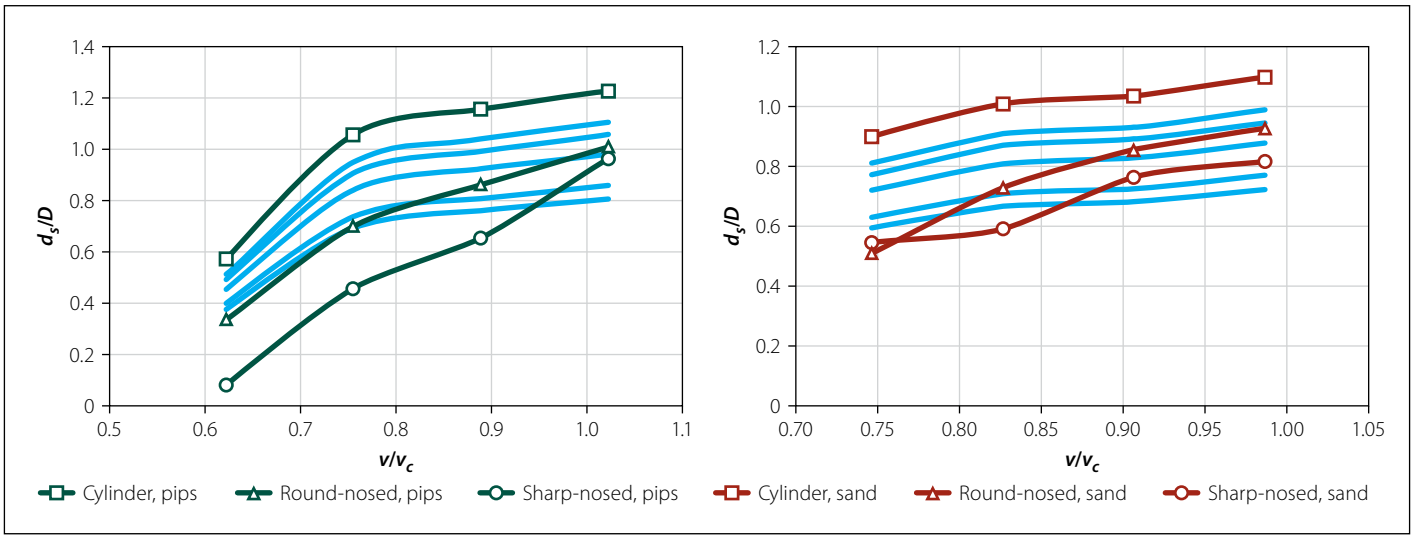

Figure 8 Evaluation of shape factors for the prediction of maximum scour depth

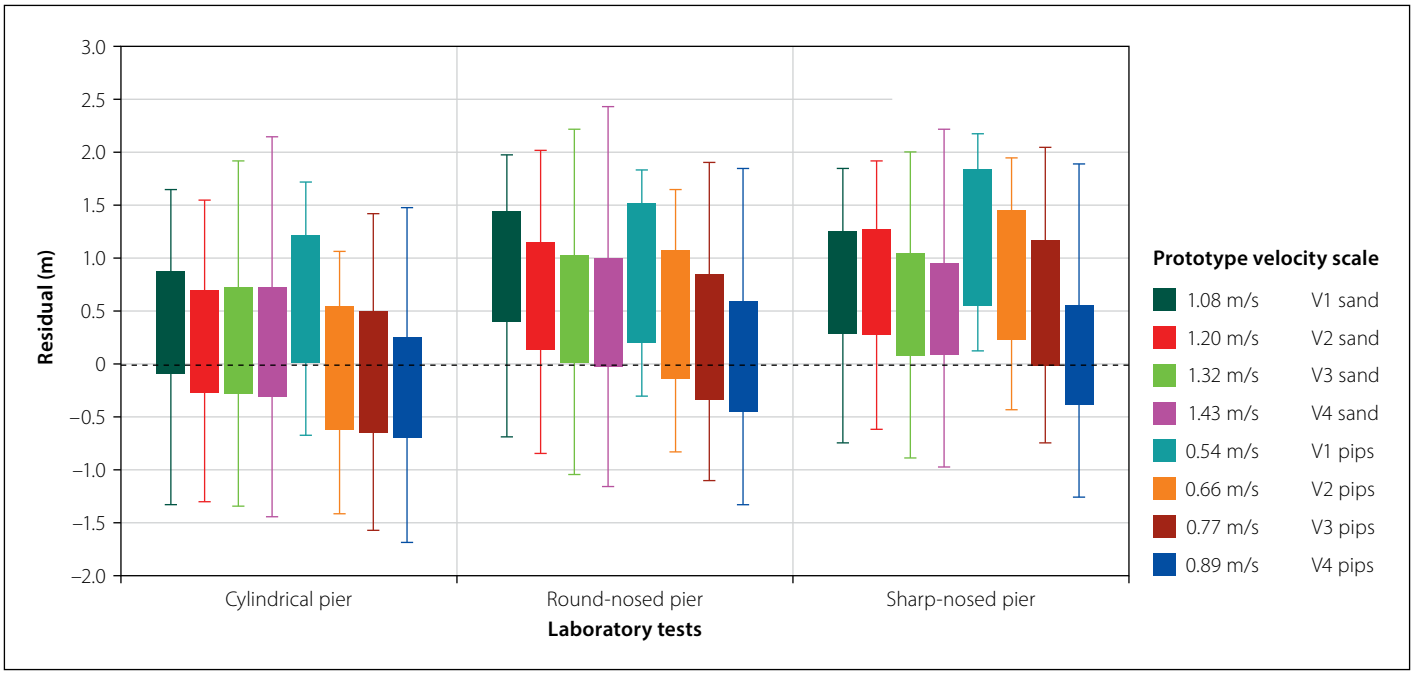

Figure 9 Boxplot showing the distribution of scour depth residuals for the different lab tests

setup with a cylindrical pier in a uniformly graded bed, the most accurate scour depths were predicted for the tests with the cylindrical pier, in addition to those with the crushed peach pips. It can be deduced that the scaling of the peach pips is a better representative of in-situ sediment behaviour than that of the fine sand. Furthermore, increased velocities yield larger scour depths and the equations yield less conservative predictions.

Similarly, the boxplots in Figure 10 compare the statistical spread for each empirical equation, which can be evaluated in conjunction with the more detailed relative scour depth dataset in Figure 11. The percentage error is given by $(d_s^{observed} - d_s^{calculated}) / d_s^{observed} \times 100$.

It is evident from Figure 10 that the equations are in weak agreement with one another and generally overestimate the observed scour depths with a mean error of 78%. The most accurate methods are those of Hancu (1971), and Melville and Kandasamy (1998a), while the safest equations for bridge pier design would be those of Blench (1969), Shen *et al* (1969) and Ali and Karim (2002), followed by the FDOT and HEC-18 equations.

In agreement with the literature study, the HEC-18 and Shen *et al* (1969) equations resembled the observed scour better. In addition, the Shen *et al* (1969) and Ali and Karim (2002) models presumably performed better because they rely on the pier Reynolds number, a parameter which has recently been identified as significant in the vortex formation by numerical model studies (Roulund *et al* 2005). The implication of this is that models taking the vortex formation into consideration could offer better scour depth predictions.

The simple Blench (1969), and Melville and Kandasamy (1998a) equations, as well as the other old models of Breusers (1965), and Laursen and Toch (1956), were more accurate despite not incorporating the approach velocity or particle size. The equations predict the same scour depth for all the tests (only Melville and Kandasamy, and Laursen and Toch are differentiated by a shape factor) and are therefore considered less applicable. Breusers is the simplest expression which assumes that the maximum bridge pier scour can be estimated at 1.4 times the pier size. Pier size is the most predominant parameter appearing in all the formulae except in the Chitale (1962) model. Subsequently, Chitale also performed deceptively well because only one pier width was tested. Instead, the Chitale and the HEC-18 formulae depend on the Froude number, which can describe the sediment bed forms and their mode of transport (Graf 1971). HEC-18 and most of the other models are also based on the relative flow depth, which can possibly describe the thickness of the boundary layer (Roulund *et al* 2005).

On the other hand, Coleman (1971) and Gao *et al* (1993), also known as the simplified Chinese equation, are not fit for pier design due to under-predictions. In accordance with preceding studies, Froelich (1988) also underestimated scour depth, and as a result the overly conservative Froelich Design equation came about, which adds the pier width to the predicted scour depth as a precautionary measure. The scour depth was also underestimated by Molinas (2004), particularly for particle sizes < 2 mm as explained by Mueller and Wagner (2005).

Kothyari, Garde and Ranga (1992) demonstrated the most significant spread of errors. It is the only identified scour model that takes sediment density into consideration and overestimates scour depth, presumably due to the challenges posed by physical model scales.

Generally, formulae developed in affiliation with Melville overestimated the scour depth more than others. These formulae, as well as the HEC-18 equations, calculate the scour depth with a simplified approach using dimensionless correction factors to account for time, channel geometry, sediment size, grade, pier shape, flow alignment, armouring, flow intensity or flow depth. The simplified approach illustrates the effect of each parameter on the scour depth, but by doing so neglects to acknowledge that the parameters are interrelated.

Furthermore, it is difficult to mathematically describe the effect of pier shape on the horseshoe vortex, and subsequently the scour depth, with simply a constant shape factor. Half of the empirical equations evaluated in this study employ different shape factors, and thus the scour depths for the round-nosed and sharp-nosed were largely overestimated, as indicated in Figure 9. Figure 10 also shows boxplots for the empirical equations

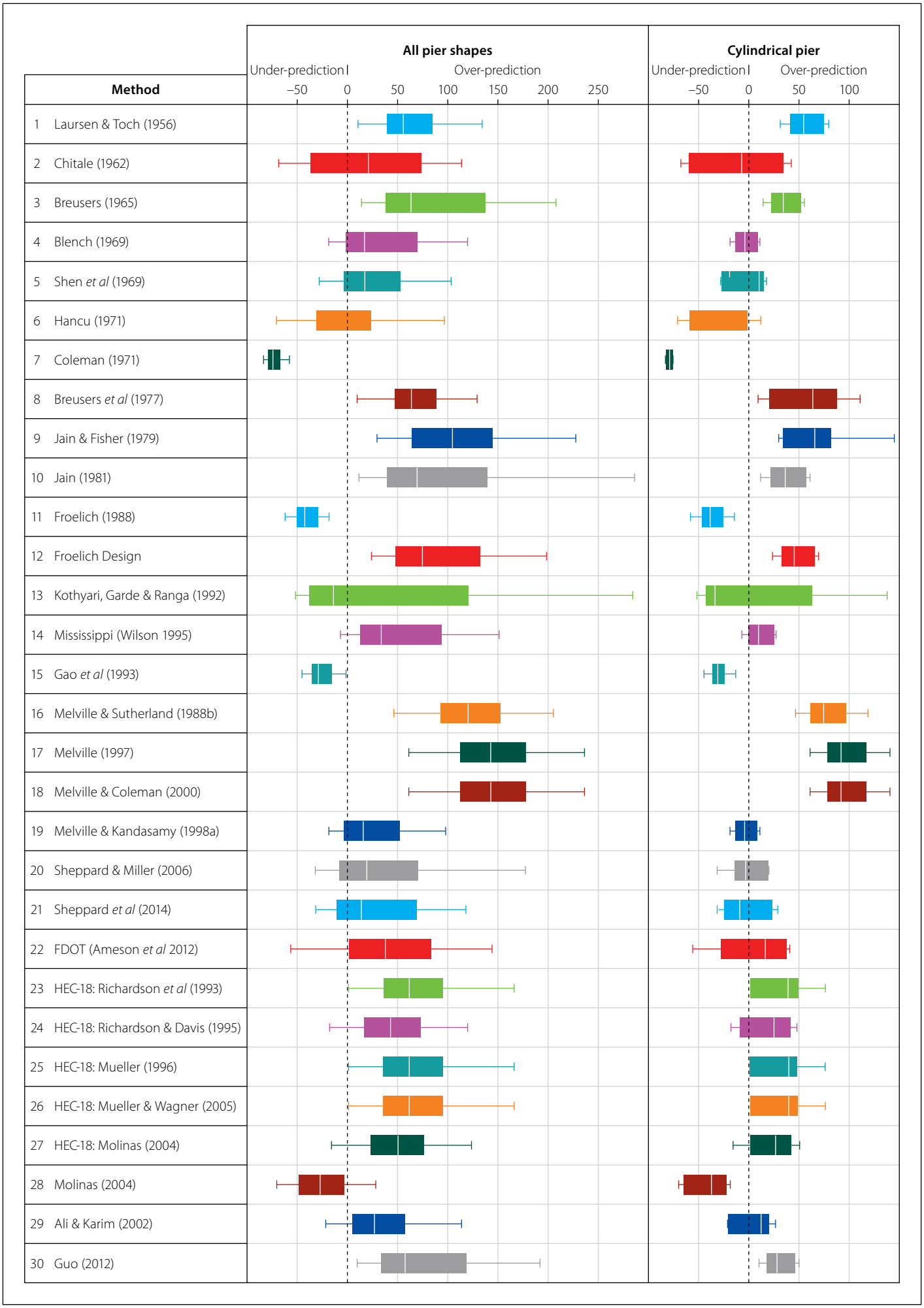

Figure 10 Boxplot showing the distribution of scour depth as a percentage error for the different empirical equations from the experimental work

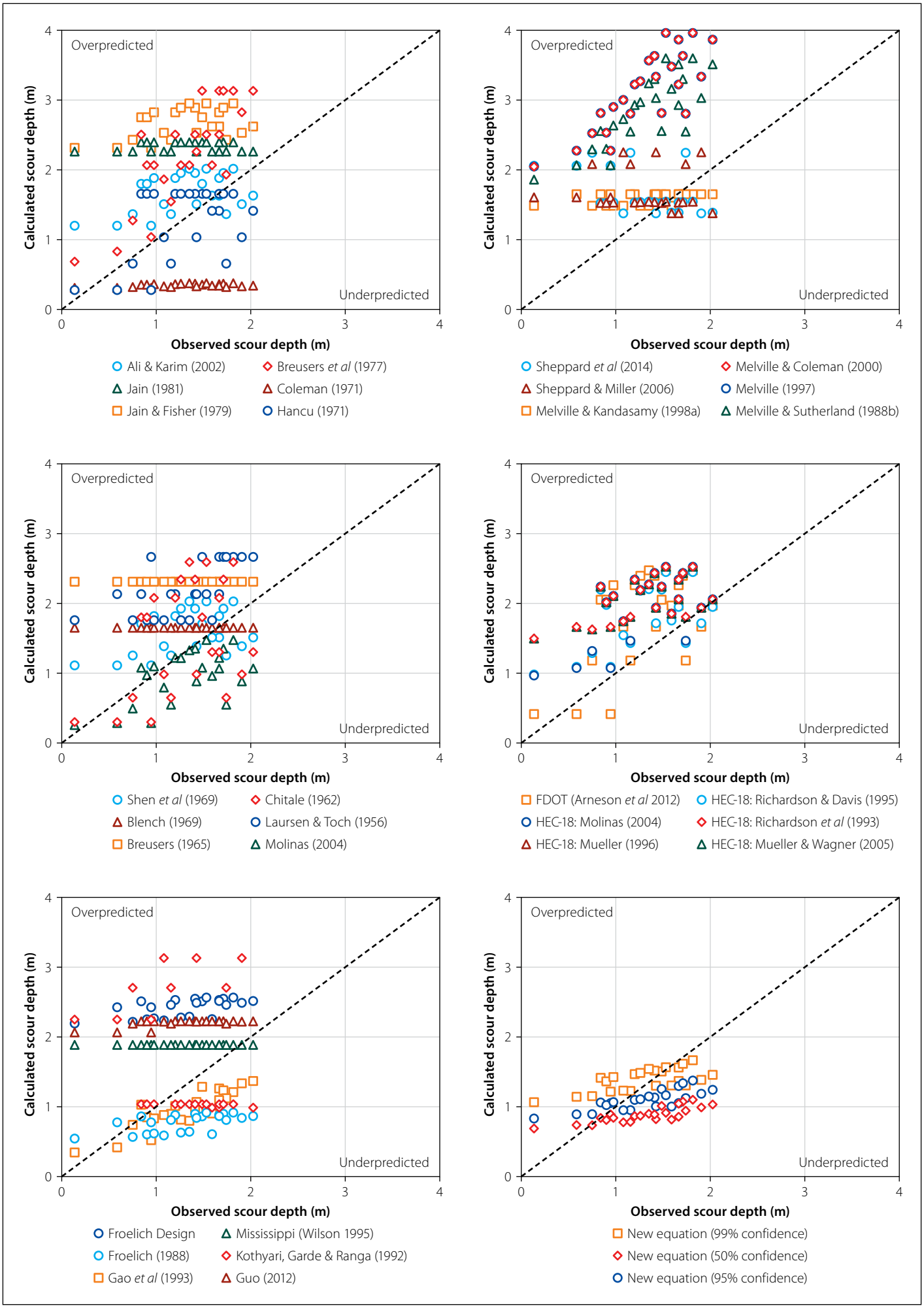

Figure 11 Comparison of relative scour depths observed from the experimental work and calculated by the different empirical equations

applied only to the cylindrical piers. The scour depths are better predicted, but they still have a mean error of 50%. The HEC-18 equations consistently performed the best, with the least under-estimations, while the other equations were inclined to over-predict less.

Five different HEC-18s have been developed with each new FHWA manual revision by improving the factor for armouring *Ka*. With the exception of Mueller and Wagner (2005), the factor *Ka* is determined by a dimensionless excess velocity intensity based on the critical velocity formulation by Gao *et al* (1993). The most recent FHWA manual discards the CSU's HEC-18 approach for the Florida DOT (Arneson *et al* 2012) based on Sheppard and Miller (2006), and Sheppard *et al* (2014) for wide piers with a new critical velocity calculation. While this method has a mean error percentage closer to zero, it also has a larger range of residuals (or higher SSR) with more under-predictions.

A new equation based on field data

Because the HEC-18 equations are generally favoured for performing better than the other empirical equations, it was attempted to further improve them by developing new dimensionless factors for armouring and pier shape. HEC-18 equations focus on the flow-structure interaction, but are limited in terms of the flow-sediment interaction (Guo 2012).

Extensive field data from the Bridge Scour Data Management System (BSDMS) (documented by Mueller and Wagner 2005) was used to perform the regression analysis. The 493 pier scour measurements were reduced to 207 measurements to satisfy the criteria for aligned flow, limited debris effects, non-cohesive sediment and upstream measurements at single piers. The measurements were also filtered to ensure the scour depths were captured within a ±0.3 m accuracy.

A new approach to bridge pier scouring was adopted whereby the unreliable critical velocity was discarded for another parameter, the particle Reynolds number *Rep*, to evaluate the erodibility of the riverbed. Other parameters were also considered, such as the movability number based on settling velocity, unit stream power and the rate of energy dissipation, but *Rep* correlated best with the relative scour depth from the field data, as shown in Figure 12 (R square = 0.84, P-value = 10^{-11}, Significance F = 10^{-61}). The correlation is given for the 50%, 95% and 99% confidence intervals that were determined statistically.

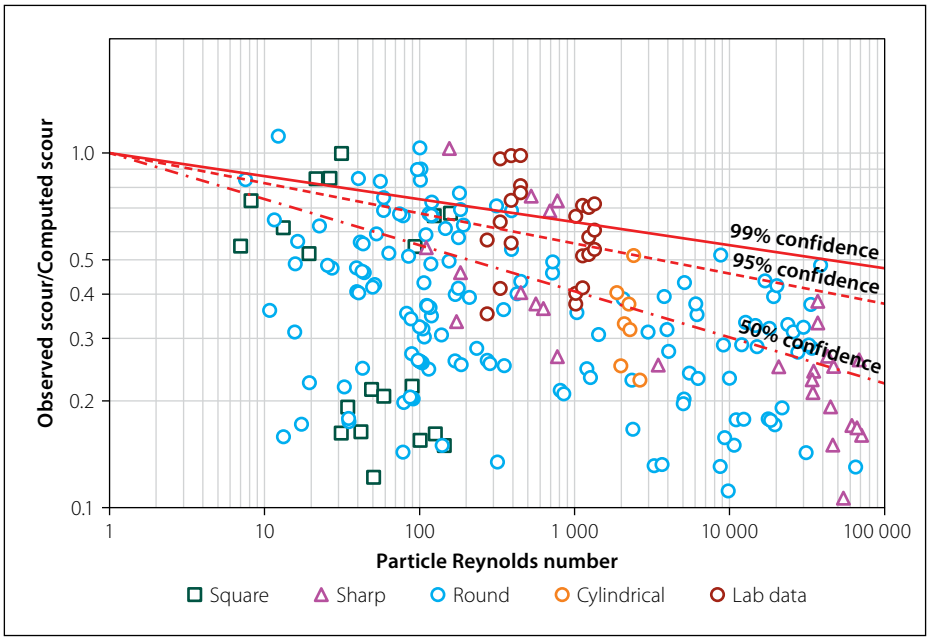

Figure 12 Relationship between the idealised factors *Ka* and *Rep*

Representative particle sizes other than the mean d_{50} were also considered in an attempt to account for the grading of the sediment bed, but the best correlation was noted for $d = d_{50}$. The particle Reynolds number has the additional benefit that it is based on the channel shape and bed form roughness. However, limited information was captured by the field data, and the energy slope S_f was determined from Chézy by assuming the hydraulic radius $R = y$ flow depth for wide channels. Bed shear stress is also based on the slope and shape of a channel, but these parameters have not been used by the models in this study to describe their effect on scour depth. Note that despite the criterion for accuracy, the field data still displays a broad scatter of data for the observed scour, even at one given site or pier where the structure and sediment parameters are fixed, that the captured flow parameters v and y alone cannot explain.

A new approach to the pier shape factor was also adopted by accounting for the relative pier lengths L/D and by employing an empirical equation whereby the effect of the pier shape on the scour depth is amplified by greater velocities, or equivalently, greater pier Reynolds numbers associated with the horseshoe vortex. Figure 13 shows that an increased shape factor correlates with the increased scour depths observed for a particle Reynolds number between 100 and 1 000.

The standard HEC-18 equation with the new proposed factors for armouring and pier shape are presented. The standard factors should be used for the bed condition with clear-water scouring $K_b = 1.1$ and for alignment $K_\theta = (\cos\theta + L/D\sin\theta)^{0.65}$. The *a* and *b* coefficients in Table 4 were determined for different confidence intervals, for while a good design equation

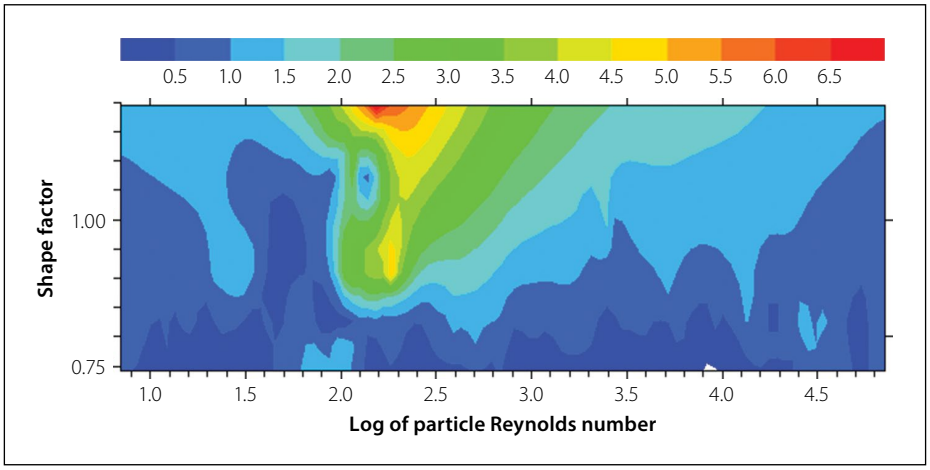

Figure 13 Contour plot for the observed bridge pier scour depth (m) relative to *Ks* and *Rep*

with a higher confidence interval may guarantee fewer under-predictions, an empirical equation with a lower confidence interval may yield more accurate predictions. Adopting a new approach with confidence intervals can quantify the trade-off between accuracy and unsafe under-predictions, offering flexibility to the bridge designer.

$$d_s = 2DK_sK_\theta K_bK_a(y_1/D)^{0.35}Fr^{0.43} \quad (5)$$

$$K_a = \left(\frac{\sqrt{gy_1S_f}\ d}{v}\right)^a \quad (6)$$

$$K_s = \begin{cases} [1.1 + 1.6E - 8(Re_D)](L/D)^b, & \text{for square-nosed piers} \\ [0.9 + 3.6E - 8(Re_D)](L/D)^b, & \text{for sharp-nosed piers} \\ (L/D)^b, & \text{for round-nosed piers} \\ 1, & \text{for cylindrical piers} \end{cases} \quad (7)$$

Table 4 New equation parameters proposed for different confidence intervals

Confidence interval	*a*	*b*
99%	−0.065	−0.03
95%	−0.095	−0.08
50%	−0.130	−0.09

As an alternative to the new proposed empirical equations, the contour plot in Figure 14, based on the Modified Liu Diagram, is capable of predicting bridge pier scour. Despite the fact that the particle Reynolds number and movability number account for all the flow and sediment parameters except for the pier structure, the observed pier scour depth in Figure 14 (not relative scour depth d_s/D) is comparable to the Modified Liu Diagram for incipient motion in Figure 3. Sediment movement is observed for *Rep* > 13 and a movability number > 0.2 in the turbulent flow region (Rooseboom *et al* 1983). The scour depth dramatically increases for a smaller particle Reynolds number between 100 and 1 000, and for a larger movability number above 3. For comparison, the scour depth calculated by the new equations 5, 6 and 7 (99% confidence) produces a smoother contour plot similar to the one observed from the field data, but with deeper scour holes in the far corner of the turbulent movement region. This new diagram relating *Rep*, *v*/w* and d_s has the potential to accurately predict bridge pier scour should it be supplemented and validated

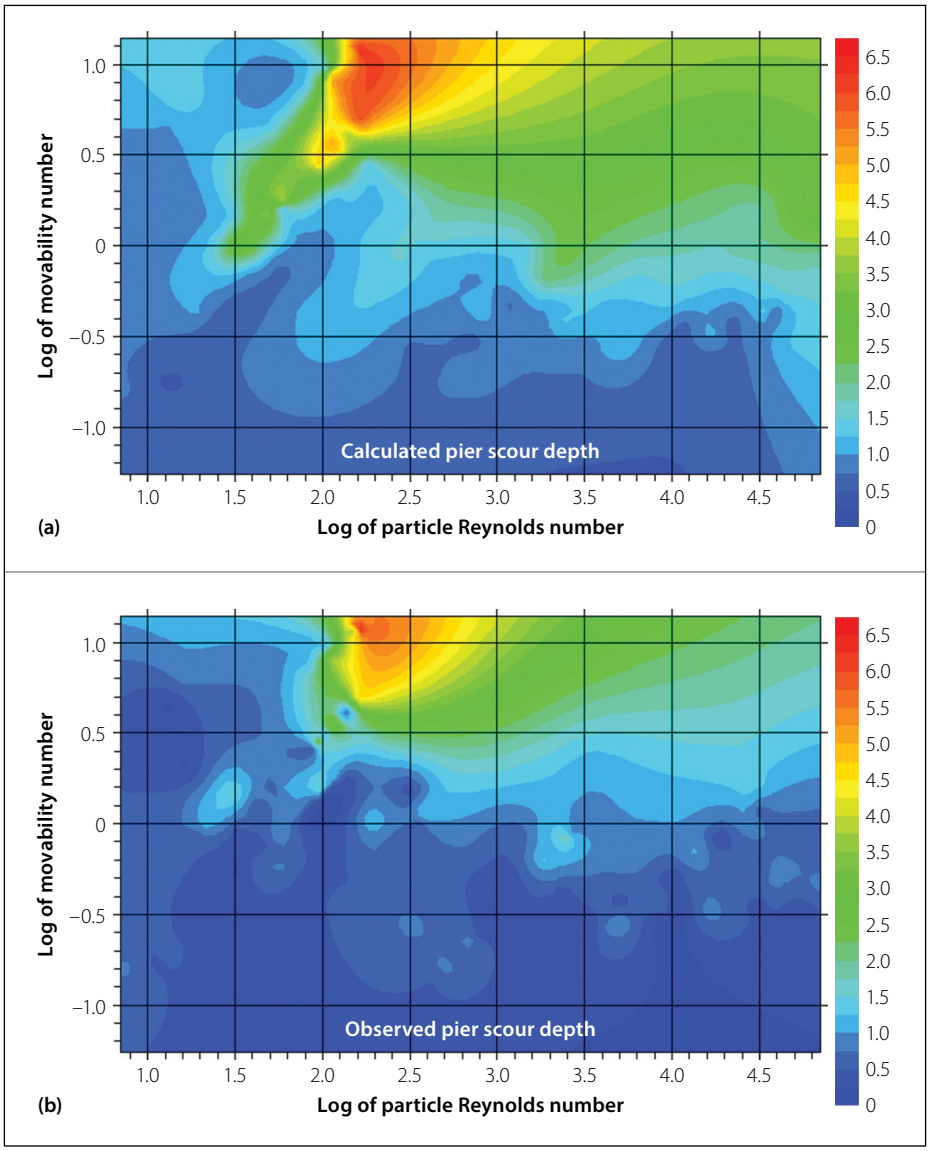

Figure 14 Modified Liu Diagram for bridge pier scour depth (m)

by additional scour data, and should the assumptions for energy slope, channel shape and settling velocity be supported.

The sum of squared residuals, as defined below, was compared against the thirty other empirical equations, for field and lab data, in Figure 15. The equations are ranked according to the least overall error and least under-predictions without any weighting. The new proposed equation ranks the highest, followed by HEC-18 Mueller (1996), Shen *et al* (1969) and Mueller and Wagner (2005) (based on *vc*, *ReD* and *d/D* respectively).

$$SSR = \sum(d_s^{computed} - d_s^{observed})2 \quad (8)$$

The new equation (99% confidence) ranked the highest with the least total SSR 186;3 and least under-predictions 1;1 for the field data and lab data combined, followed by the new equation with the 95% and 50% confidence intervals for the combined data. It also had the least total SSR 3 and the second least under-predictions of SSR 1 for the lab data. The new equation (50% confidence) yielded the least total SSR 71 followed by 94 for the new equation (95% confidence) for just the field data (ranking 11th and 15th in under-predictions). For the lab data, the new equation (95% confidence) ranked second and third, and the new equation (50% confidence) ranked fourth and sixth in the least total SSR and under-predictions respectively.

If the ±0.3 m accuracy of the pier scour measurements is considered, the SSR for the field data is 12 and for the lab data is 0. The new equation (95% confidence) is therefore also adequately reliable as a design equation (with an SSR for under-predictions of 10 less than the 12 representing the accuracy of the data).

The new proposed equation performs comparably better to the field data than to the lab data. The new equations have achieved considerably less scatter about the line of equality, despite under-predictions

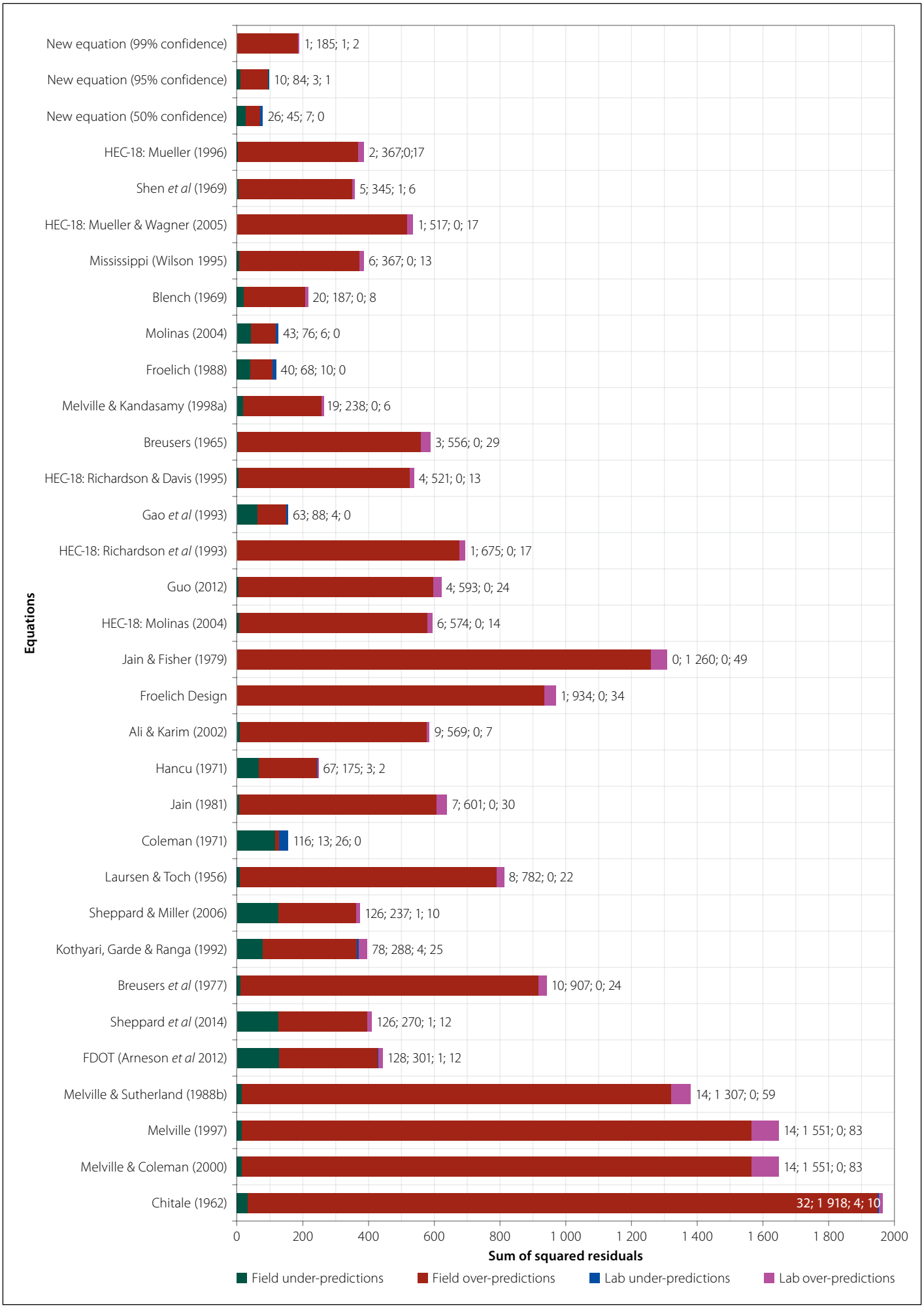

Figure 15 Comparison of the sum of squared residuals for the different equations for lab data and field data

for the cylindrical piers. The new equation (50% confidence) would not be fit for pier design due to under-predictions, but the new equation (99% confidence) is the most accurate method that has a compact boxplot range of error and a mean error percentage closest to but greater than zero (10%) and a minimum of only –28% (acceptable compared to the lab error of 9%).

TRANSITION TOWARDS NUMERICAL MODELLING

Evidently, the scouring process at the riverbed interface is complex and affected by numerous interrelated parameters (Rooseboom 2013). Various attempts have been made to address the complexity by assuming dominant variables and reducing them to simplified relationships to describe scour. However, it is difficult to generalise the scour process, because there are so many interrelated variables that may conceal the influence of one another on scouring. Furthermore, simplifying assumptions are required to quantify the three-dimensional flow patterns, complicated vortex and turbulence structures. These limit the extent to which a mathematical analysis can be made to model scour (Tseng *et al* 2000; Guo 2012). When faced with such uncertainty in bridge design, hydraulic engineers are compelled to pursue costly, labour-intensive and time-consuming physical model studies, which have their own flow visualisation and scaling challenges (Xiong *et al* 2014).

Most sediment studies are still based on empirical formulae derived and calibrated by means of a coefficient from small-scale laboratory experiments, and occasionally field data, despite the availability of sophisticated computers. More weight should be attached to relationships that are fundamentally sound and based on first principles, such as the conservation of mass and momentum, which computer software is capable of solving (Olsen & Malaaen 1993). A recently studied alternative is the use of three-dimensional numerical models to better predict equilibrium scour depth.

Numerical solutions by Computation Fluid Dynamics (CFD) are becoming increasingly popular to compute fluid flow as technology advances and the cost of computational time decreases. Hydrodynamic models coupled with sediment transport algorithms have the ability to predict not only scour depth, but also scour geometry (such as l_s and w_s from Table 3). Furthermore, they are not limited in terms of scale restrictions (Sawadogo 2015) and allow parametric studies of conditions that are otherwise impossible or difficult to investigate in the laboratory (Sumer 2007).

However, numerical models are not without limitations – for example, computer constraints in terms of memory capacity and processors, as well as the computational effort (Sawadogo 2015). The accuracy of the solution relies on the underlying assumptions of governing sediment transport equations and the model's ability to resolve the vortices (Abbasnia & Ghiassi 2011). Although extensive research has been conducted for more than six decades, comparatively little research has been presented on numerical modelling of bridge pier scour (Baykal *et al* 2015). Most of these numerical models focus on resolving the flow and horseshoe vortex, particularly for a flat rigid bed, and not on modelling scour.

Olsen and Melaaen (1993), and in a follow-up study Olsen and Kjellesvig (1998) were the first to attempt simulating bridge pier scour with a numerical model by employing convection-diffusion and bed load equations. The results compared fine with empirical formulae, but the simulation took nine weeks to solve 80×10^3 cells, and the horseshoe vortex was not resolved. In more recent studies, Khosronejad *et al* (2012) and Xiong *et al* (2014) developed numerical models, but these also significantly under-predicted the scour pattern at the pier nose because the horseshoe vortex was not properly resolved. Roulund *et al* (2005), and in a follow-up study Baykal *et al* (2015), have shown the most promising results whereby the upstream scour depth agrees well with their experimental work, but a discrepancy of up to 30% was observed for the scour pattern downstream of the pier.

Finally, it may be interesting to note that, unlike the other models, the equation for bridge pier scour by Ali and Karim (2002) was developed from a numerical model for the associated complex flow field.

CONCLUSIONS AND RECOMMENDATIONS

Traditional methods for estimating the maximum scour depth near bridge piers rely on simplistic formulae, each with its own assumptions and limitations, which often yield unreliable results. Thirty of these empirical equations were evaluated for their ability to predict bridge pier scour, and their shortcomings were thereby demonstrated. In accordance with previous studies, it was confirmed that the equations are in weak agreement with one another. They produce a wide range of errors relative to one another (in the order of 95%), because the equations are not universal and only yield good results under conditions similar to those from which they were derived.

Because the empirical equations are generally developed from a standard experimental setup with a cylindrical pier in a uniformly graded bed, the most accurate scour depths were predicted for the tests with the cylindrical pier. Only half of the empirical equations evaluated in this study account for other pier shapes by incorporating a constant shape factor. However, the effect of the pier shape on scouring cannot simply be described by a single dimensionless shape factor or constant.

Furthermore, the scour holes were better predicted for the tests with crushed peach pips than those with a fine sand bed. It can be deduced that the scaling of the peach pips by the movability number is a better representative of in-situ sediment behaviour, and that the non-scalable effects of the hydraulic forces in the settling velocity and density can be overcome by using a sediment with a smaller density and larger particle size (Heller 2011).

The scour depth was predominantly over-predicted by the equations while those of Coleman (1971), Froelich (1988) and Gao *et al* (1993) are not fit for pier design due to recurrent under-predictions. While the over-prediction of the observed scour may cause one to query the equilibrium time, two hours have been the basis for the derivation of several equations and are justified by Melville (1975), Roulund *et al* (2005), Mohammed *et al* (2016) and Guo (2014).

Most of the empirical equations for bridge pier scour are reliant on the selection of an appropriate critical velocity. Hancu (1971) proves to be the most accurate scour prediction model for the lab data, presumably because it relies on a critical velocity that is derived from Shields and the sediment density.

No single equation is conclusively the best, but the HEC-18 models appeared to consistently perform better in safely predicting the observed lab and field scour depths for all pier shapes, in agreement with Mueller and Wagner (2005), Gaudio *et al* (2010) and Toth (2015). Generally, the HEC-18 model is favoured by the US FHWA engineers for field results that are least likely to be under-predicted (Arneson *et al* 2012). In

addition, the equations of Shen *et al* (1969), and Ali and Karim (2002) are recommended for conceptual design, because they rely on the pier Reynolds number, a parameter which has been identified as significant in the horseshoe vortex and subsequent scour hole formation. Prediction models taking the vortex formation into consideration could offer better scour depth predictions.

Finally, field data was analysed to improve the standard HEC-18 equation with new factors for armouring and pier shape. The pier shape accounts for *L/D* and uses a linear equation whereby the effect of the pier shape on the scour depth is amplified by greater pier Reynolds numbers. The new armouring factor is based on the particle Reynolds number as opposed to the widely adopted critical velocity, and achieves considerably less scatter about the line of equality despite under-predictions for the cylindrical piers. A new approach with confidence intervals was adopted to quantify the trade-off between accuracy and under-predictions, offering flexibility to the bridge designer.

The new equation (99% confidence) ranked the highest with the least total SSR and least under-prediction for the scour depths from the field data and lab data combined, followed by HEC-18 Mueller (1996), Shen *et al* (1969), and Mueller and Wagner (2005). If the accuracy of the field pier scour measurements is considered, the new equation (95% confidence) is also adequately reliable as a design equation, while the new equation (50% confidence) would not be fit for bridge design due to under-predictions of the equilibrium bridge pier scour depth. The new proposed equation performs comparably better to the field data than to the lab data. However, it still has the lowest mean error percentage to the other methods of 10%, which is acceptable compared to the lab error of 9%.

As an alternative to the new proposed empirical equations, the diagram in Figure 14 relating *Rep*, *v*/w* and *ds* is comparable to the Modified Liu Diagram for incipient motion and has the potential to predict bridge pier scour, even though the pier structure parameters are omitted.

The simplicity of conservative empirical equations may be appealing; nonetheless, overestimating the anticipated scour depth leads to uneconomical designs with unnecessarily expensive foundations and countermeasures. Further research and improved prediction models should be considered, particularly advanced CFD numerical models which are becoming increasingly feasible. In short, numerical modelling should be the primary subject of future studies. Numerical models have led to an improved understanding of the flow mechanisms and scour process, which could ultimately lead to improved scour equations derived from first principles and not empirically.

ACKNOWLEDGEMENT

The financial assistance of the National Research Foundation (NRF) towards this research is hereby acknowledged with gratitude. The opinions expressed, and conclusions arrived at, are those of the authors and should not be attributed to the NRF.

APPENDIX

List of empirical equations

d_s = Bridge pier scour depth
ρ = Fluid density
ρ_s = Sediment density
v = Kinematic viscosity
t = Time
D = Pier diameter or width
L = Pier length
d = Median sediment size
σ_g = Particle size distribution
s = Specific gravity
v_1 = Approach flow velocity
y_1 = Approach flow depth
g = Gravitational acceleration
v_c = Sediment critical velocity
Fr = Froude number
α = Angle of flow in radians
B = Channel width
K_s = Shape factor

1	Laursen & Toch (1956)	$d_s = 1.35D^{0.7}y_1^{0.3}K_s$ Square K_s = 1.1; Circular K_s = 1; Round K_s = 0.8; Sharp K_s = 0.66
2	Chitale (1962)	$d_s = y_1(6.65Fr - 0.51 - 5.49Fr^2)$
3	Breusers (1965)	$d_s = 1.4D$
4	Blench (1969)	$d_s = 1.8y_1^{0.75}D^{0.25} - y_1$
5	Shen *et al* (1969)	$d_s = 0.00023(v_1D/v)^{0.619}$
6	Hancu (1971)	$d_s = 2.42D\left(\frac{2v_1}{v_c} - 1\right)\left(\frac{v_1}{gD}\right)^{1/3}$ for $0.5 < \frac{v_1}{v_c} < 1$ $v_c = 1.2\sqrt{gd(s-1)}(y_1/d)^{0.2}$
7	Coleman (1971)	$\frac{v_1}{\sqrt{2gd_s}} = 0.6\left(\frac{v_1}{D}\right)^{0.9}$
8	Breusers *et al* (1977)	$d_s = D\left(\frac{2v_1}{v_c} - 1\right)\left[2\tan h\left(\frac{y_1}{D}\right)\right]K_sK_\theta$ for $0.5 < \frac{v_1}{v_c} < 1$ Square K_s = 1.1; Circular K_s = 1; Round K_s = 0.8; Sharp K_s = 0.66 Assume v_c from Neill's formulation (1973)

9	Jain & Fisher (1979)	$d_{s1} = 2D(Fr_1 - Fr_c)^{0.25}\left(\frac{y_1}{D}\right)^{0.5}$ for $(Fr - Fr_c) > 0.2$ $d_{s2} = 1.85DFr_1^{0.25}\left(\frac{y_1}{D}\right)^{0.5}$ for $(Fr - Fr_c) < 0$ $d_s = \max(d_{s1}, d_{s2})$ for $0 < (Fr - Fr_c) < 0.2$ $Fr_c = \frac{v_c}{\sqrt{gy_1}}$ Assume v_c from Neill's formulation (1973)
10	Jain (1981)	$d_s = 1.84y_1Fr_c^{0.25}\left(\frac{D}{y_1}\right)^{0.7}$ Assume v_c from Neill's formulation (1973)
11a	Froelich (1988)	$d_s = 0.32K_sD^{0.62}y_1^{0.47}Fr^{0.22}d^{-0.09}$ Square $K_s = 1.3$; Circular $K_s = 1$; Round $K_s = 1$; Sharp $K_s = 0.7$
11b	Froelich Design	$d_s = 0.32K_sD^{0.62}y_1^{0.47}Fr^{0.22}d^{-0.09} + D$
12	Kothyari, Garde & Ranga (1992)	$d_s = \left(\frac{D}{d}\right)^{-0.25}\left(\frac{y_1}{D}\right)^{0.16}\left(\frac{v_1^2 - v_c^2}{(s-1)gd}\right)^{0.4}$ for $\frac{v_1}{v_c} < 1$ $v_c^2 = 1.2[(s-1)gd]\left(\frac{D}{d}\right)^{-0.11}\left(\frac{y_1}{d}\right)^{0.16}$
13	Mississippi (Wilson 1995)	$d_s = 0.9D^{0.6}y_1^{0.4}$
14	Simplified Chinese Gao *et al* (1993)	$d_s = 0.46K_sD^{0.6}y_1^{0.15}d^{-0.07}\left(\frac{v_1 - v_i}{v_c - v_i}\right)^{\eta}$ $\eta = \left(\frac{v_c}{v_1}\right)^{9.35+2.23\log(d)}$ $v_c = \left(\frac{y_1}{d}\right)^{0.14}\left[17.6(s-1)d + 6.05E^{-7}\left(\frac{10 + 0.3048y_1}{(0.3048d)^{0.72}}\right)\right]^{0.5}$ $v_i = 0.645v_c\left(\frac{d}{D}\right)^{0.053}$ Square $K_s = 1.1$; Circular $K_s = 1$; Round $K_s = 0.8$; Sharp $K_s = 0.66$
15	Melville & Sutherland (1988b)	$d_s = K_\theta K_\sigma K_s K_{y1}(2.4K_I)K_d$ Gradation factor $K\sigma = 1$
	Alignment factor	$K_\theta = \left(\cos\theta + \frac{L}{D\sin\theta}\right)^{0.65}$
	General shape factor	Square $K_s = 1.1$; Circular $K_s = 1$; Round $K_s = 1$; Sharp $K_s = 0.9$
	Flow intensity factor	$K_1 = \frac{v_1 - (v_a - v_c)}{v_c}$ for $\frac{v_1 - (v_a - v_c)}{v_c} < 1$ $K_I = 1$ for $\frac{v_1 - (v_a - v_c)}{v_c} \geq 1$ $u_c^* = 0.0115 + 0.0125d^{1.4}$ for 0.1 mm < d < 1 mm $u_c^* = 0.0305d^{0.5} + 0.0065d^{-1}$ for 1 mm < d < 100 mm Median armour size $d_a = \frac{d_{max}}{1.8}$ for $v_a = 0.8v_{ca}$ $v_{ca} = 5.75u_{ca}^*\left[\log\left(5.53\frac{y_1}{d_a}\right)\right]$ $v_c = 5.75u_c^*\left[\log\left(5.53\frac{y_1}{d}\right)\right]$

	Sediment factor	$K_d = 0.57 \log\left(2.24\frac{D}{d}\right)$ for $\frac{D}{d} \leq 25$ $K_d = 1$ for $\frac{D}{d} > 25$
	Depth size factor	$K_{y1} = D$ for $\frac{y_1}{D} > 2.6$ $K_{y1} = 0.78D\left(\frac{y_1}{D}\right)^{0.255}$ for $\frac{y_1}{D} < 2.6$
16	Melville (1997)	$d_s = K_\theta K_G K_s K_y K_I K_a$ Channel geometry $K_G = 1$ for a bridge pier
	Revised depth size factor	$K_y = 2.4D$ for $\frac{D}{y_1} < 0.7$ $K_y = 2\sqrt{y_1 D}$ for $0.7 < \frac{D}{y_1} < 5$ $K_y = 4.5y_1$ for $\frac{D}{y_1} > 5$
17	Melville & Coleman (2000)	$d_s = K_\theta K_G K_s K_y K_I K_d K_t$ Time factor $K_t = \exp\left[-0.07\frac{v_c}{v_1}\left\lvert ln\left(\frac{t}{t_e}\right)\right\rvert^{1.5}\right]$ for $\frac{v_1}{v_c} < 1$ where t_e = total time to reach equilibrium profile
18	Melville & Kandasamy (1998a)	$d_s = K_s K y_1^n D^{1-n}$ $K = 5$, $n = 1$ for $0.04 \geq \frac{y_1}{D}$ $K = 1$, $n = 0.5$ for $0.04 < \frac{y_1}{D} < 1$ $K = 1$, $n = 0$ for $\frac{y_1}{D} \geq 1$
19	Sheppard & Miller (2006)	$d_s = 2.5Df_1f_2f_3$ for $0.47 < \frac{v_1}{v_c} < 1$ $f_1 = \tanh\left[\left(\frac{y_1}{D}\right)^{0.4}\right]$ $f_2 = \left\{1 - 1.75\left[ln\left(\frac{v_1}{v_c}\right)\right]^2\right\}$ Assume v_c from Neill's formulation (1973) $f_1 = \frac{\frac{D}{d}}{0.4\left(\frac{D}{d}\right)^{1.2} + 10.6\left(\frac{D}{d}\right)^{-0.13}}$
20	Sheppard *et al* (2014)	$d_s = 2.5Df_1f_2f_3K_1D$ for $0.4 \leq \frac{v_1}{v_c} < 1.0$ $f_1 = \tanh\left[\left(\frac{y_1}{K_1D}\right)^{0.4}\right]$ $f_2 = \left\{1 - 1.2\left[ln\left(\frac{v_1}{v_c}\right)\right]^2\right\}$ $f_3 = \left(\frac{K_1D}{d}\right)\left[0.4\left(\frac{K_1D}{d}\right)^{1.2} + 10.6\left(\frac{K_1D}{d}\right)^{-0.13}\right]^{-1}$ $K_1 = 1$ for cylindrical piers $K_1 = 0.86 + 0.97\left(\alpha - \frac{\pi}{4}\right)^4$ for rectangular piers

	Sheppard *et al* (2014) (continued)	$u_c^* = \left\{16.2d\left[\frac{9.09 \times 10^{-6}}{d} - d\left(38.76 + 9.6ln(d)\right) - 0.005\right]\right\}^{1/2}$ $Re = \frac{u_c^* d}{v}$ for $5 \le Re \le 70$ $v_c = 2.5u_c^* d\ ln\left\{73.5\frac{y_1}{d}\left[Re\left(2.85 - 0.58ln(Re) + 0.002Re\right) + \frac{111}{Re} - 6\right]^{-1}\right\}$ for $Re > 70$ $v_c = 2.5u_c^*\ ln\left(\frac{2.21y_1}{d}\right)$ for $Re < 70$
21	FDOT (Arneson *et al* 2012)	$d_s = 2.5f_1f_2f_3K_1D$ for $0.4 < \frac{v_1}{v_c} \le 1.0$ $v_c = 2.5u_c^* \log\left(5.53\frac{y_1}{d}\right)$ $u_c^* = 0.0377 + 0.041d^{1.4}$ for 0.1 mm < d < 1 mm $u_c^* = 0.1d^{0.5} - \frac{0.0213}{d}$ for 1 mm < d < 100 mm
22	HEC-18 or CSU equations	$d_s = 2.5DK_sK_\theta K_bK_a\left(\frac{y_1}{D}\right)^{0.35} Fr^{0.43}$ Bed condition factor $K_b = 1.1$ for clear-water scouring
22a	Richardson *et al* (1993)	Armouring factor $K_a = 1$
22b	Richardson & Davis (1995)	$K_a = [1 - 0.89(1 - V_R)^2]^{0.5}$ Dimensionless excess velocity intensity $V_R = \frac{v_1 - v_i}{v_{c90} - v_i}$ $v_i = 0.645v_c\left(\frac{d}{D}\right)^{0.053}$ $v_{c90} = 6.19y_1^{1/6}d_{90}^{1/3}$ where $d_{90} = d\sigma_g^{1.282}$
22c	Mueller (1996)	$K_a = 0.4V_R^{0.15}$ $V_R = \frac{v_1 - v_i}{v_c - v_{i95}}$ $v_i = 0.645v_c\left(\frac{d}{D}\right)^{0.053}$ $v_{i95} = 0.645\ v_{c95}\left(\frac{d_{95}}{D}\right)^{0.053}$ where $d_{95} = d\sigma_g^{1.645}$
	Critical velocity (Neill 1973)	$v_c = \theta_s^{0.5}31.08y_1^{1/6}d^{1/3}$ using Shields parameter $\theta_s = 0.0019d^{-0.384}$ if d < 0.0009 m $\theta_s = 0.0942d^{0.175}$ if 0.0009 m < d < 0.020 m $\theta_s = 0.047$ if d > 0.020 m
22d	Mueller & Wagner (2005)	$K_a = 0.35\left(\frac{D}{d}\right)^{0.19}$
22e	Molinas (2004)	$K_a = 1.25 + 3\sqrt{\frac{d_{cfm}}{d}}V_R^{0.6}ln(V_R + 0.5)$ $V_R = \frac{v_1 - v_i}{v_{cm} - v_i}$ $v_i = 2.65y_1^{1/6}\ d_{35}{}^{1/3}$ $v_{cm} = 6.625y_1^{1/6}\ d_{cfm}{}^{1/3}$ $d_{cfm} = \frac{d_{85} + 2d_{90} + 2d_{95} + d_{99}}{6}$

23	Molinas (2004)	$d_s = 0.99K_iK_sK_\theta K_bK_aV_R^{0.55}D^{0.66}y^{0.17}$ Scour initiation $K_i = \left(1 - \frac{v_i}{v_1}\right)^{0.45}$ $\text{Ka} = 1.25 + 3\sqrt{\frac{d_{cfm}}{d}}V_R^{0.6}ln(V_R + 0.5)$
24	Ali & Karim (2002)	$d_s = \frac{K_1D_*^{1.2}y_1}{\left(\frac{v_1D}{v}\right)}\left[1 - \text{Exp}\left(-5.32E^{-4}\frac{v_1t}{y_1}\right)\right]$ $\text{K1} = 0.1\sqrt{(s-1)g}d^{3/2}D_*^{-0.3}$ $D_* = [(s-1)gv^{-2}]^{1/3}$
25	Guo (2012)	$\text{ds} = \sqrt{Dy}\tanh\left(\frac{H^2}{3.75\sigma_g}\right)$ where $\sigma_g = \sqrt{\frac{d_{84}}{d_{16}}}$ Densiometric particle Froude number $H = \frac{v_1}{\sqrt{(s-1)gd}}$

REFERENCES

Abbasnia, A H & Ghiassi, R 2011. Improvements on bed-shear stress formulation for pier scour computation. *International Journal for Numerical Methods in Fluids*, 67, 383–402.

Ali, K H M & Karim, O A 2002. Simulation of flow around piers. *Journal of Hydraulic Research*, 40(2): 161–174.

Arneson, L A, Zevenbergen, L W, Lagasse, P F & Clopper, P E 2012. *Evaluating scour at bridges*. Report FHWA-HIF-12-003. Washington, DC: US Department of Transportation, Federal Highway Administration.

Baykal, C, Sumer, B M, Fuhrman, D R, Jacobsen, N G & Fredsøe, J 2015. Numerical investigation of flow and scour around a vertical circular cylindrical pier. *Philosophical Transactions of the Royal Society A*, 373(2033).

Blench, T 1969. *Mobile-bed fluviology*. Edmonton, Canada: University of Alberta Press.

Breusers, H N C 1965. Scour around drilling platforms. *Bulletin of Hydraulic Research*, 19: 276.

Breusers, H N C, Nicollet, G & Shen, H W 1977. Local scour around cylindrical pier. *Journal of Hydraulic Research*, 15(3): 211–252.

Chitale, S V 1962. Scour at bridge crossings. *Transactions of the American Society of Civil Engineers*, 127(1): 191–196.

Coleman, N L 1971. Analyzing laboratory measurements of scour at cylindrical piers in sand beds. *Proceedings,* 14th Congress of the International Association for Hydraulic Research (IAHR), 29 August – 3 September, Paris, Vol 3, pp 307–313.

Deshmukh, A R & Raikar, R V 2014. A clear-water scour around a circular bridge pier under steady flow for different opening ratios. *International Journal of Research in Engineering and Technology*, 3(1): 158–162.

Ettema, R 1980. *Scour at bridge piers*. Auckland, New Zealand: University of Auckland, Department of Civil Engineering.

Froelich, D C 1988. Analysis of onsite measurements of scour at piers. *Proceedings,* ASCE National Conference on Hydraulic Engineering, 8–10 August, Colorado Springs, CO, pp 534–539.

Gao, D, Posada, G L & Nordin, C F 1993. *Pier scour equations used in the People's Republic of China*. Report FHWA-SA-93-076. Washington, DC: US Department of Transportation, Federal Highway Administration.

Gaudio, R, Grimaldi, C, Tafarojnoruz, A & Calomino, F 2010. Comparison of formula for the prediction of scour depth at piers. *Proceedings,* 1st International Association for Hydraulic Research (IAHR) Congress, 4–6 May, Edinburgh.

Graf, W H 1971. *Hydraulics of Sediment Transport. (Series in Water Resources and Environmental Engineering)*. New York: McGraw-Hill.

Guo, J 2012. Pier scour in clear water for sediment mixtures. *Journal of Hydraulic Research*, 50(1): 18–27.

Guo, J 2014. Semi-analytical model for temporal clear water scour at prototype piers. *Journal of Hydraulic Research*, 52(3): 366–374.

Hancu, S 1971. On the estimation of local scour in the bridge piers zone. *Proceedings,* 14th International Association for Hydraulic Research (IAHR) Congress, 20–22 November, Delft, Netherlands, Vol 3, pp 299–313.

Heller, V 2011. Scale effects in physical hydraulic engineering models. *Journal of Hydraulic Research*, 49(3): 293–306.

Huber, F 1991. Update: Bridge scour. *ASCE Civil Engineering*, 61(9): 62–63.

Jain, S C & Fischer, E E 1979. *Scour around circular piers at high Froude numbers*. Report FHWA-RD-79-104. Washington, DC: US Department of Transportation, Federal Highway Administration.

Jain, S C 1981. Maximum clear-water scour around circular piers. *ASCE Journal of the Hydraulics Division*, 107(HY5): 611–626.

Johnson, P A 1995. Comparison of pier-scour equations using field data. *ASCE Journal of Hydraulic Engineering*, 121(8): 626–629.

Khosronejad, A, Kang, S & Sotiropoulos, F 2012. Experimental and computational investigation of local scour around bridge piers. *Advances in Water Resources*, 37: 73–85.

Kothyari, U C, Garde, R C J & Ranga Raju, K G 1992. Temporal variation of scour around circular bridge piers. *ASCE Journal of Hydraulic Engineering*, 118(8): 1091–1106.

Landers, M N & Mueller, D S 1996. Evaluation of selected pier-scour equations using field data. *Transportation Research Record*, 1523: 186–195.

Laursen, E M & Toch, A 1956. *Scour around bridge piers and abutments*. Bulletin No. 4, Ames, IA: Iowa Highway Research Board.

Lee, S O & Strum, T W 2009. Effect of sediment size scaling on physical modelling of bridge pier scour. *ASCE Journal of Hydraulic Engineering*, 135(10): 793–802.

Melville, B W 1975. *Local scour at bridge site*. Report No. 117. Auckland, New Zealand: University of Auckland, School of Engineering.

Melville, B W & Chiew, Y M 1999. Time scale for local scour at bridge piers. *ASCE Journal of Hydraulic Engineering*, 125(1): 59–65.

Melville, B W & Coleman, S E 2000. *Bridge scour*. Highlands Ranch, CO: Water Resources Publications.

Melville, B W & Kandasamy, J K 1998a. Maximum local scour depth at bridge piers and abutments. *ASCE Journal of Hydraulic Research*, 26(2): 183–198.

Melville, B W & Sutherland, A J 1988b. Design methods for local scour at bridge piers. *ASCE Journal of Hydraulic Engineering*, 114(10): 1210–1226.

Melville, B W 1997. Pier and abutment scour: Integrated approach. *ASCE Journal of Hydraulic Engineering*, 123(2): 125–136.

Mohammed, Y A, Abdel-Aal, G M, Nasr-Allah, T H & Shawky, A A 2016. Experimental and theoretical investigations of scour at bridge abutment. *Journal of King Saud University – Engineering Sciences*, 28(1): 32–40.

Molinas, A 2004. *Bridge scour in nonuniform sediment mixtures and in cohesive materials*. Report FHWA-RD-03-083. Washington, DC: US Department of Transportation, Federal Highway Administration.

Mueller, D S & Wagner, C R 2005. *Field observations and evaluations of streambed scour at bridges*. Report FHWA-RD-03-052. Washington, DC: US Department of Transportation, Federal Highway Administration.

Mueller, D S 1996. *Local scour at bridge piers in nonuniform sediment under dynamic conditions*. PhD thesis. Fort Collins, CO: Colorado State University.

Neill, C R 1973. *Guide to bridge hydraulics*. Toronto, Canada: University of Toronto Press.

Olsen, N R B & Kjellesvig, H M 1998. Three-dimensional numerical flow modelling for estimation of maximum local scour depth. *Journal of Hydraulic Resources*, 36(4): 579–590.

Olsen, N R B & Melaaen, M C 1993. Three-dimensional calculation of scour around cylindrical piers. *ASCE Journal of Hydraulic Engineering*, 119(9): 1048–1054.

Richardson, E V & Davies, S R 1995. *Evaluating scour at bridges*, 3rd ed. Report FHWA-IP-90-017. Washington, DC: US Department of Transportation, Federal Highway Administration.

Richardson, E V, Harrison, L J, Richardson, J R & Davis, S R 1993. *Evaluating scour at bridges,* 2nd ed. Report FHWA-IP-90-017. Washington, DC: US Department of Transportation, Federal Highway Administration.

Rooseboom, A 2013. *Drainage Manual*, 6th ed. Chapter 8. Pretoria: SANRAL.

Rooseboom, A, Basson, M S, Loots, C H, Wiggett, J H & Bosman, J 1983. *National Transport Commission Road Drainage Manual*, 2nd ed. Pretoria: Director-General: Transport, Chief Directorate: National Roads.

Roulund, A, Sumer, B M, Fredsøe, J & Michelsen, J 2005. Numerical and experimental investigation of flow and scour around a circular pile. *Journal of Fluid Mechanics*, 524: 351–401.

Sawadogo, O 2015. *Coupled fully three-dimensional mathematical modelling of sediment deposition and erosion in reservoirs*. PhD thesis. Stellenbosch University, Department of Water Engineering.

Shen, H W, Schneider, V R & Karaki, S 1969. Local scour around bridge piers. *ASCE Journal of the Hydraulics Division*, 95(6): 1919–1940.

Sheppard, D M & Miller, W 2006. Live-bed local pier scour experiments. *Journal of Hydraulic Engineering*, 132(7): 635–642.

Sheppard, D M, Melville, B & Demir, H 2014. Evaluation of existing equations for local scour at bridge piers. *Journal of Hydraulic Engineering*, 140(1): 14–23.

Sumer, B M 2007. Mathematical modelling of scour: A review. *Journal of Hydraulic Research*, 45(6): 723–735.

Toth, E 2015. Asymmetric error functions for reducing the underestimation of local scour around bridge piers. *Journal of Hydraulic Engineering,* 141(7): 04015011.

Tseng, M H, Yen, C L & Song, C C S 2000. Computation of three-dimensional flow around square and circular piers. *International Journal for Numerical Methods in Fluids*, 34: 207–227.

Van Rijn, L C 1987. *Mathematical modelling of morphological processes in the case of suspended sediment transport*. PhD thesis. Delft University of Technology, Netherlands.

Williams, P D 2014. *Scale effects on design estimation of scour depths at piers*. PhD thesis. Stellenbosch University, Department of Civil Engineering.

Wilson, K V 1995. *Scour at selected bridge sites in Mississippi*. Water-Resources Investigations Report 94–4241. Reston, VA: US Geological Survey.

Xiong, W, Cai, C S, Kong, B & Kong, X 2014. CFD simulations and analyses for bridge scour development using a dynamic mesh updating technique. *Journal of Computing in Civil Engineering*, 30(1): 1–11.

Zanke, U 1977. Berechnung der Sinkgeschwindigkeiten von Sedimenten. [Calculation of the sinking velocity of sediments.] *Mitteilungen des Franzius-Instituts für Wasserbau*, 46(243): 231–245.